Microbiome

RESEARCH

Open Access

Akkermansia muciniphila improve cognitive dysfunction by regulating BDNF and serotonin pathway in gut-liver-brain axis

Eun Ji Kang[1†], Min-Gi Cha[2†], Goo-Hyun Kwon[2†], Sang Hak Han[3], Sang Jun Yoon[2], Sang Kyu Lee[4], Moo Eob Ahn[5], Sung-Min Won[2*†], Eun Hee Ahn[1,6*†] and Ki Tae Suk[2*†]

Abstract

Backrground *Akkermansia muciniphila*, a next-generation probiotic, is known as a cornerstone regulating the gut-organ axis in various diseases, but the underlying mechanism remains poorly understood. Here, we revealed the neuronal and antifibrotic effects of *A. muciniphila* on the gut-liver-brain axis in liver injury.

Results To investigate neurologic dysfunction and characteristic gut microbiotas, we performed a cirrhosis cohort (154 patients with or without hepatic encephalopathy) and a community cognition cohort (80 participants in one region for three years) and validated the existence of cognitive impairment in a 3,5-diethoxycarbonyl-1,4-dihydrocollidine-induced hepatic injury mouse model. The effects of the candidate strain on cognition were evaluated in animal models of liver injury. The expression of brain-derived neurotrophic factor (BDNF) and serotonin receptors was accessed in patients with fibrosis (100 patients) according to the fibrosis grade and hepatic venous pressure gradient. The proportion of *A. muciniphila* decreased in populations with hepatic encephalopathy and cognitive dysfunction. Tissue staining techniques confirmed gut-liver-brain damage in liver injury, with drastic expression of BDNF and serotonin in the gut and brain. The administration of *A. muciniphila* significantly reduced tissue damage and improved cognitive dysfunction and the expression of BDNF and serotonin. Isolated vagus nerve staining showed a recovery of serotonin expression without affecting the dopamine pathway. Conversely, in liver tissue, the inhibition of injury through the suppression of serotonin receptor (5-hydroxytryptamine 2A and 2B) expression was confirmed. The severity of liver injury was correlated with the abundance of serotonin, BDNF, and *A. muciniphila*.

Conclusions *A. muciniphila,* a next-generation probiotic, is a therapeutic candidate for alleviating the symptoms of liver fibrosis and cognitive impairment.

Keywords *Akkermansia muciniphila*, BDNF, Serotonin, Gut-organ axis, Liver injury, Cognitive impairment

[†]Eun Ji Kang, Min-Gi Cha, Goo-Hyun Kwon, Sung-Min Won, Eun Hee Ahn and Ki Tae Suk contributed equally to this work.

*Correspondence:
Sung-Min Won
lionbanana87@hallym.ac.kr
Eun Hee Ahn
eunhee.ahn@hallym.ac.kr
Ki Tae Suk
ktsuk@hallym.ac.kr
Full list of author information is available at the end of the article

Graphical Abstract

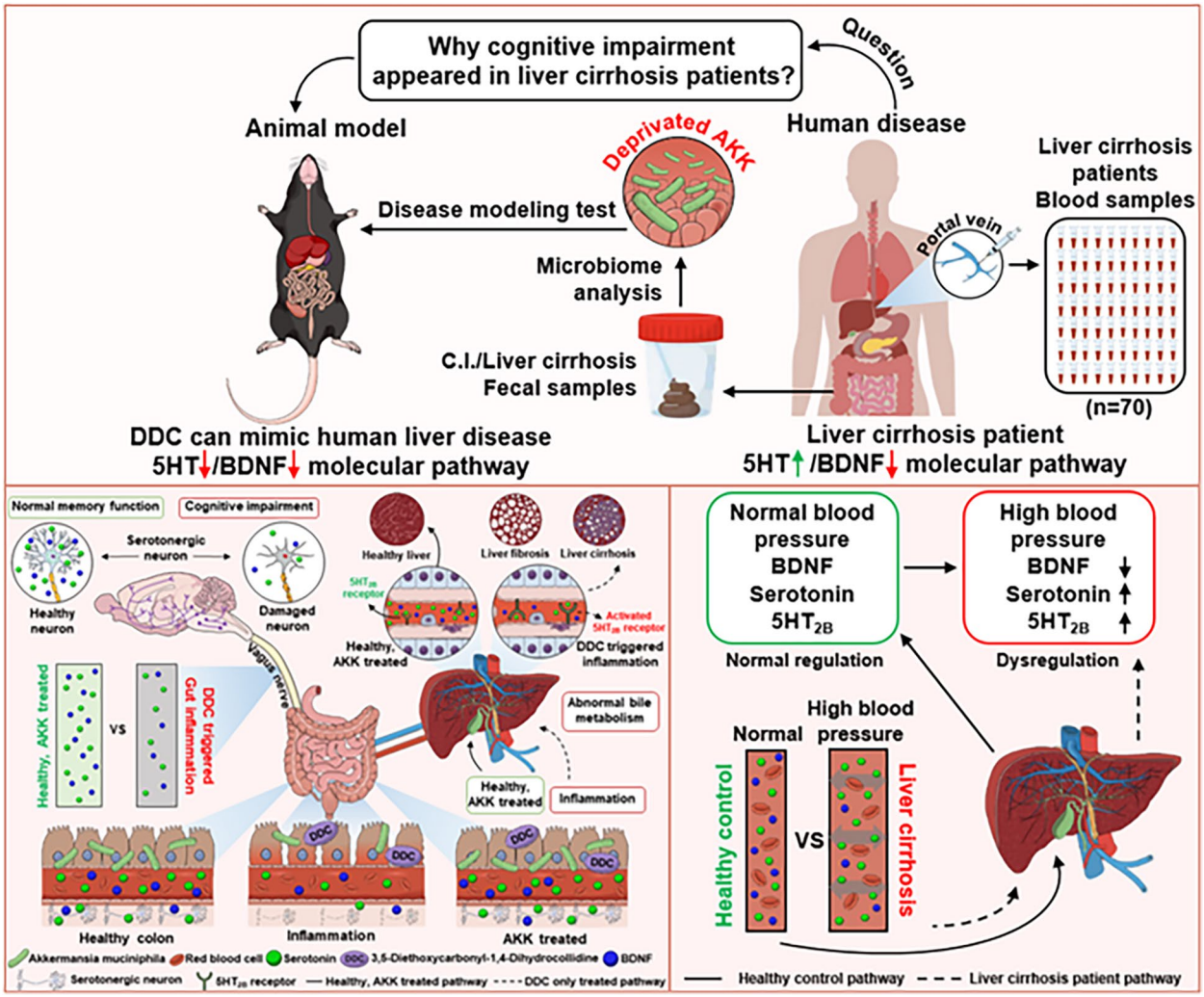

Background

Hepatic encephalopathy (HE) is a neuropsychiatric syndrome that occurs in patients with acute or chronic liver disease and involves a wide range of cognitive and psychiatric impairments [1–3]. HE is a serious complication of decompensated liver cirrhosis and is associated with dysbiosis or an altered gut microbiota that contributes to a systemic inflammatory environment [4, 5]. Patients with liver cirrhosis exhibit atrophic changes in the frontal lobe and a neuronal loss in the cerebral cortex, hypothalamus, and hippocampus, which are responsible for impaired cognitive function [6]. The strong link between brain-related cirrhosis complications and the gut microbiome indicated by the ability of rifaximin, a nonabsorbable antibacterial agent, to maintain remission in HE patients [3, 7].

However, the role and relationship between the gut microbiota and neuropsychiatric factors in liver cirrhosis are still unclear, and the mechanisms involved in the gut-liver-brain axis flow remain to be elucidated. Investigating which neurotransmitter molecules are connected through the gut-organ axis is necessary to understand the neuropsychiatric abnormalities commonly found in cirrhotic patients and to find cures.

Akkermansia muciniphila is an anaerobic commensal bacterium that utilizes mucins as a source of carbon and nitrogen [8, 9]. Numerous studies have shown that the abundance of this commensal bacterium is associated with multiple diseases [10, 11]. *A. muciniphila* enhances intestinal barrier function and mucus layer thickness while reducing systemic endotoxin concentrations in

Table 1 Comparison of clinical parameters among healthy control, cirrhosis without encephalopathy and cirrhosis with encephalopathy

Characteristics	Healthy control (*n* = 57)	Cirrhosis without HE (*n* = 58)	Cirrhosis with HE (*n* = 39)	*P*-value
Age, *y*	61.7 ± 1.0	58.5 ± 1.6	63.2 ± 2.2	0.23 $^{n.s}$
Sex (male [%])	30 (53)	45 (78)	23 (59)	
BMI, kg/m^2	23.9 ± 0.6	23.5 ± 0.6	23.7 ± 0.5	0.87 $^{n.s}$
ALT, *U/L*	22.8 ± 1.2^{a}	72.3 ± 30.0^{b}	21.2 ± 2.1^{a}	0.0009 **
AST, *U/L*	25.0 ± 0.8^{a}	103.5 ± 21.8^{b}	51.7 ± 5.2^{bc}	< 0.0001 **
GGT, *U/L*	39.9 ± 5.5^{a}	390.5 ± 94.5^{b}	76.1 ± 21.4^{a}	< 0.0001 **
Total cholesterol, *mg/dL*	190.4 ± 5.1^{a}	133.5 ± 6.4^{b}	106.8 ± 6.2^{c}	< 0.0001 **
Creatine, *mg/dL*	0.9 ± 0.1	0.8 ± 0.0	1.0 ± 0.1	0.23 $^{n.s}$
Triglyceride, *mg/dL*	154.4 ± 17.4^{a}	134.6 ± 16.6^{a}	74.9 ± 9.0^{b}	< 0.0001 **
HDL, *mg/dL*	54.6 ± 2.8^{a}	46.4 ± 3.9^{b}	32.1 ± 2.9^{b}	< 0.0001 **

Data are represented as mean ± SEM. Different superscript letters indicates significant difference by the nonparametric Kruskal–Wallis test with Dunn's multiple comparison test. * $P < 0.05$, ** $P < 0.01$, n.s., not significant

HE Hepatic encephalopathy, *ALT* Alanine transaminase, *AST* Aspartate transaminase, *GGT* Gamma-glutamyl trans-ferase, *HDL* High-Density Lipoprotein Cholesterol

a high-fat diet-fed mouse model [10]. The administration of *A. muciniphila* to an animal model of alcoholic liver disease prevented liver injury, steatosis, and neutrophil infiltration, preserved the mucus thickness, and protected against ethanol-induced gut leakage [12]. The effects of this bacterium on enhancing intestinal barrier immune function and improving metabolic diseases in animal models have been investigated in various studies, and the effects have also been verified through recent proof-of-concept clinical trials [13]. Recently, *A. muciniphila* was shown to modulate serotonin secretion and metabolism in the gut [14, 15].

Both serotonin and brain-derived neurotrophic factor (BDNF) are important molecules that play significant roles in the pathophysiology of various neuropsychiatric disorders, including dementia and cirrhosis. BDNF is a neurotrophic factor that supports the survival and growth of neurons, and it is critical for neuroplasticity, learning, and memory. Moreover, BDNF is highly expressed in gut enteric neurons and glia and is involved in regulating various gastrointestinal functions, including motility and secretion [16]. Previous studies have shown that BDNF levels are decreased in patients with Alzheimer's disease and Parkinson's disease, and this decrease is associated with cognitive impairment and motor dysfunction [17, 18]. In addition, studies have also shown a reduction in BDNF levels in patients with cirrhosis, and this decrease is associated with HE, a condition that is characterized by cognitive dysfunction [19].

Similarly, serotonin is expressed in enteric neurons and acts as a neurotransmitter and a hormone in the gastrointestinal tract. Serotonin is a neurotransmitter that is involved in various physiological processes, including mood regulation, cognition, and memory. Previous studies have shown that serotonin levels are altered in patients with dementia and cirrhosis. Specifically, reduced serotonin levels have been observed in patients with Alzheimer's disease, which are associated with cognitive impairment [20]. In patients with cirrhosis, alterations in serotonin signaling have been implicated in the development of HE [21, 22].

Although previous scientific experiments have confirmed that BDNF and serotonin are important molecules involved in cognitive impairment and hepatitis, the exact molecular mechanisms involved have not been identified to date. Therefore, we used various animal models of liver injury to analyze the correlation between advanced liver injury and cognitive impairment and to identify novel molecular mechanisms involving BDNF/serotonin and the microbiome. We also evaluated the therapeutic effects of the next generation of beneficial microbes, specifically *A. muciniphila*, on liver injury and cognitive impairment.

Materials and methods

Human study

A hospital-based cohort study was conducted at university hospitals to evaluate the microbial characteristics of patients with cirrhosis (trial registration: NCT05786755, NCT04339725, and IRB No. 2016–134). A total of 154 patients (aged > 40 years and with alcohol-related liver cirrhosis) were included in this study. The clinical data are presented in Table 1. HE was diagnosed when overt symptoms of West Haven criteria 1–2 were present. Patients without overt symptoms (West Haven criteria 0) were classified as having no HE.

We performed brain CT scan and tests of neuropsychological function, including attention, language, visuospatial, verbal memory, visual memory, and frontal/executive function [Seoul Neuropsychological Screening Battery (SNSB)]. Patients with HE showed atrophic changes in the frontal lobe, the main region for cognitive function, and cognitive dysfunction in the neuropsychological function tests.

In the community cognition cohort study, 80 patients were enrolled to evaluate cognitive function between January 2020 and December 2022 (trial registration: cris KCT0008315 and IRB No. 2020–09-005). Cognitive function was measured in patients with memory loss in a certain area for three years (Supplementary Table 1). We conducted this cohort study on participants (age > 65 years) who did not have any psychoneurological diseases. Participants had no problems in daily life and cognitive dysfunction was diagnosed through the CERAD-K (Korean version of the Consortium to Establish a Registry for Alzheimer's Disease Assessment Packet, Neuropsychological Assessment Collection).

Patients were classified through liver biopsy and hepatic venous pressure gradient (HVPG) using data from a previous study. Liver biopsy specimens were sent to 1 center and analyzed by 2 hepatopathologists. The fibrosis stage was determined using the METAVIR staging system: 0, no fibrosis; 1, enlarged fibrotic portal tracts; 2, enlargement of portal tracts with rare periportal or portal-portal septa; 3, numerous septa without cirrhosis; and 4, cirrhosis. Advanced fibrosis is defined by METAVIR score 3–4. HVPG was measured by one hepatologist. A 6 French balloon catheter was placed in the right hepatic vein through a right jugular vein puncture for measurement of the free hepatic venous pressure. The wedged hepatic venous pressure was measured by inflating the balloon catheter in the right hepatic vein. Then, the HVPG was determined by subtracting the free hepatic venous pressure from the wedged hepatic venous pressure [23]. An HVPG ≥ 5 mmHg indicates portal hypertension, and a value exceeding 10 mmHg indicating clinically significant portal hypertension. At values greater than 12 mm Hg, variceal hemorrhage may occur [24]. We divided patients into three groups: stage 1, HVPG ≤ 5; stage 2, 5 < HVPG ≤ 15; stage 3, HVPG > 15.

The study protocols conformed to the ethical guidelines of the 1975 Declaration of Helsinki as reflected in the a priori approval by the institutional review board for human research of all participating hospitals. Informed consent for participation in the study was obtained from each patient.

Baseline evaluations were conducted, which included the family history and history of alcohol consumption, abdominal ultrasound or contrast-enhanced computed tomography, X-ray, electrocardiography, complete blood count, electrolytes, liver function test, viral markers, and endoscopy. Blood was analyzed using standard methodologies. Serum biochemical parameters included bilirubin, aspartate aminotransferase (AST), alanine aminotransferase (ALT), gamma glutamyl transpeptidase, alkaline phosphatase, albumin, sodium, total bilirubin, prothrombin time, total protein, blood glucose, international normalized ratio and total cholesterol levels. The levels of HAV (anti-HAV IgG and IgM), HBV (anti-HBc IgM, HBsAg, and anti-HBs), anti-HEV IgG and IgM, HIV, and HCV (anti-HCV with/without HCV-RNA) were tested in all patients. CMV, EBV, HSV, anti-nuclear antibody, anti-mitochondrial antibody, and anti-smooth muscle antibody tests were also performed. All experiments using human blood samples complied with relevant ethical regulations.

Animal study

Five-week-old pathogen-free male C57BL/6 J mice were obtained from Doo Yeol Biotech (Seoul, Republic of Korea). All mice were housed in individual cages maintained at 24 °C ± 2 °C on a 12 h light/dark cycle. Throughout the experiment, water and food were provided ad libitum, and the animals were monitored daily. The experimental design included an adaptation period for all groups, during which the mice were fed a normal diet for one week.

Mice were fed normal chow (Doo Yeol Biotech, Seoul, Republic of Korea) or a diet containing 3,5-diethoxycarbonyl-1,4-dihydrocollidine (DDC, 2018S, Doo Yeol Biotech, Seoul, Republic of Korea). The antibiotic cocktail combinations [ampicillin (100 mg/kg, Sigma-Aldrich, Germany), vancomycin (50 mg/kg, Sigma-Aldrich, Germany), metronidazole (100 mg/kg, Sigma-Aldrich, Germany), neomycin (100 mg/kg, Sigma-Aldrich, Germany), and amphotericin B (1 mg/kg, Supelco, Germany)] were used according to a previously reported method [25]. Sarpogrelate hydrochloride, which is an antagonist for 5HTR2A/2B, was administered orally at a dose of 50 mg/kg BW every 2 days. After one week of adaptation, six-week-old male C57BL/6 J mice underwent bile duct ligation (BDL) surgery. Under anesthesia, the abdominal cavity was opened, and the bile duct was ligated twice with 5–0 surgical silk. The bile duct was cut between the ligatures. Sham surgery was performed similarly, except that ligation and dissection of the bile duct were not performed. Oral administration of the bacterial strain was performed beginning 1 week after BDL surgery. The bacterial strain was orally administered 3 times a week at a concentration of approximately 10^9 CFU/ml in 200 µl. The mice were eventually sacrificed via an overdose of inhalation anesthesia with isoflurane (Hana Pharm,

Seoul, Republic of Korea) at the conclusion of the treatment period.

Mice were treated humanely, and all aspects of the animal study were performed in accordance with National Institutes of Health Guidelines for the Care and Use of Laboratory Animals. All experimental procedures were approved by the Institutional Animal Care and Use Committee of the College of Medicine, Hallym University (Hallym 2022–53).

Microbiome analysis

Metagenomic DNA was extracted using a QIAamp stool kit (Qiagen, Hilden, Germany). After the first amplification of the V3—V4 region of the bacterial 16S rRNA gene, the second amplification was performed using Barcoded universal primers. An Agencourt AMPure XP system (Beckman, USA) was used to purify amplicons. PicoGreen and quantitative PCR were utilized to quantify the purified amplicons. After pooling barcoded amplicons, a MiSeq sequencer on the Illumina platform (CJ bioscience Inc., Republic of Korea) was used for sequencing according to the manufacturer's specifications. The 16S-based Microbial Taxonomic Profiling platform of EzBioCloud Apps (CJ bioscience Inc., Republic of Korea) was used for microbiome profiling. After taxonomic profiling of each sample, a comparative analysis of the samples was performed by comparison with the EzBioCloud database. The 16S rRNA database (DB ver. PKSSU4.0) of CJ bioscience was used for the taxonomic assignment of reads. OTU picking was achieved with UCLUST [26] and CDHIT utilizing a 97% similarity cutoff [27]. Beta-diversity, which includes PCoA and UPGMA clustering, was displayed in the comparative MTP analyzer.

Refer to the supplementary data for details about other materials and methods.

Results

A. muciniphila is drastically depleted from the fecal microbiome of human subjects with diseases associated with cognitive dysfunction

The study included 97 patients diagnosed with liver cirrhosis (without HE, $n=58$; with HE, $n=39$) and 57 healthy controls. In addition, 48 cognitively impaired subjects (Mini-Mental State Examination [MMSE]-KC score ≤ 24) and 32 healthy controls (MMSE-KC score ≥ 25) classified by an examination of the MMSE score were included. Table 1 and Table S1 present the detailed characteristics of each group, including clinical, metabolic, and biochemical profiles. Cirrhotic patients with HE had lower levels of ALT ($P=0.0009$) (Supplementary Fig. 1A), AST ($P<0.0001$) (Supplementary Fig. 1A), gamma-glutamyl transferase ($P<0.0001$), total cholesterol ($P<0.0001$), and triglycerides ($P<0.0001$) than cirrhotic patients without HE. No differences in blood biochemical profiles were observed between the test groups classified using the MMSE.

We analyzed 16S rRNA gene sequencing data to compare the distribution of microbe proportions according to the presence or absence of disease. The proportions of dominant taxa at the phylum (Fig. 1A) and family levels are shown (Supplementary Fig. 1B). Significant differences in the overall proportions were observed between the healthy control group and the cirrhotic group. We confirmed that the abundance of *Bacteroidetes* decreased ($P<0.0001$); conversely, the abundance of *Proteobacteria* ($P<0.0001$) and *Actinobacteria* ($P=0.033$) increased in the fecal samples from the cirrhosis group with or without HE (Fig. 1A). In addition, at the family level, *Ruminococcaceae* ($P<0.0001$), *Lachnospiraceae* ($P=0.0007$), and *Prevotellaceae* ($P<0.0001$) were depleted, but *Enterococcaceae* ($P=0.052$) and *Lactobacillaceae* ($P=0.0065$) levels were elevated (Supplementary Fig. 1A). Alpha diversity was determined based on the Chao1, ACE and Shannon metrics (Fig. 1B and Supplementary Fig. 1C). Compared to the healthy control group, all the cirrhotic groups exhibited significant decreases ($P<0.01$) in species richness (Chao1 and ACE) and diversity indices (Shannon). In terms of differences between the cirrhotic groups with and without HE, a decrease in the diversity indices of the in cirrhotic patients with HE was observed (Chao1, $P=0.0014$; ACE, $P=0.0009$; Shannon, $P=0.025$). We confirmed the abundance of specific taxa according to differences in liver diseases (Fig. 1C). *Ruminococcaceae* ($P<0.0001$) and *Lachnospiraceae* ($P<0.0001$) were significantly decreased in fecal samples from the cirrhotic patient group. Moreover, we also analyzed which species varied by patient group, and particular strain in the gut microbiota was *A. muciniphila* ($P=0.0039$).

We performed a 16S rRNA gene sequencing analysis of fecal samples from patients with cognitive impairment to understand the cognitive impairment symptoms in cirrhotic patients. No significant differences in alpha diversity or taxon proportions at the phylum and family levels were detected between the healthy control and cognitive impairment groups (Fig. 1D and E, Supplementary Fig. 1D, and 1E). Interestingly, we observed that the abundance of *A. muciniphila* was reduced ($P=0.032$) in the cognitive impairment patient group but not in the healthy control group, which was consistent with the 16S rRNA sequencing results from the fecal samples of the cirrhotic patients (Fig. 1F). Hence, a positive correlation ($R=0.015$; $P=0.09$) was observed between the abundance of *A. muciniphila* and the MMSE-KC score, which is a criterion for cognitive impairment (Fig. 1G). In linear discriminant effect size analysis (LEfSe) performed to confirm differences in bacterial community composition

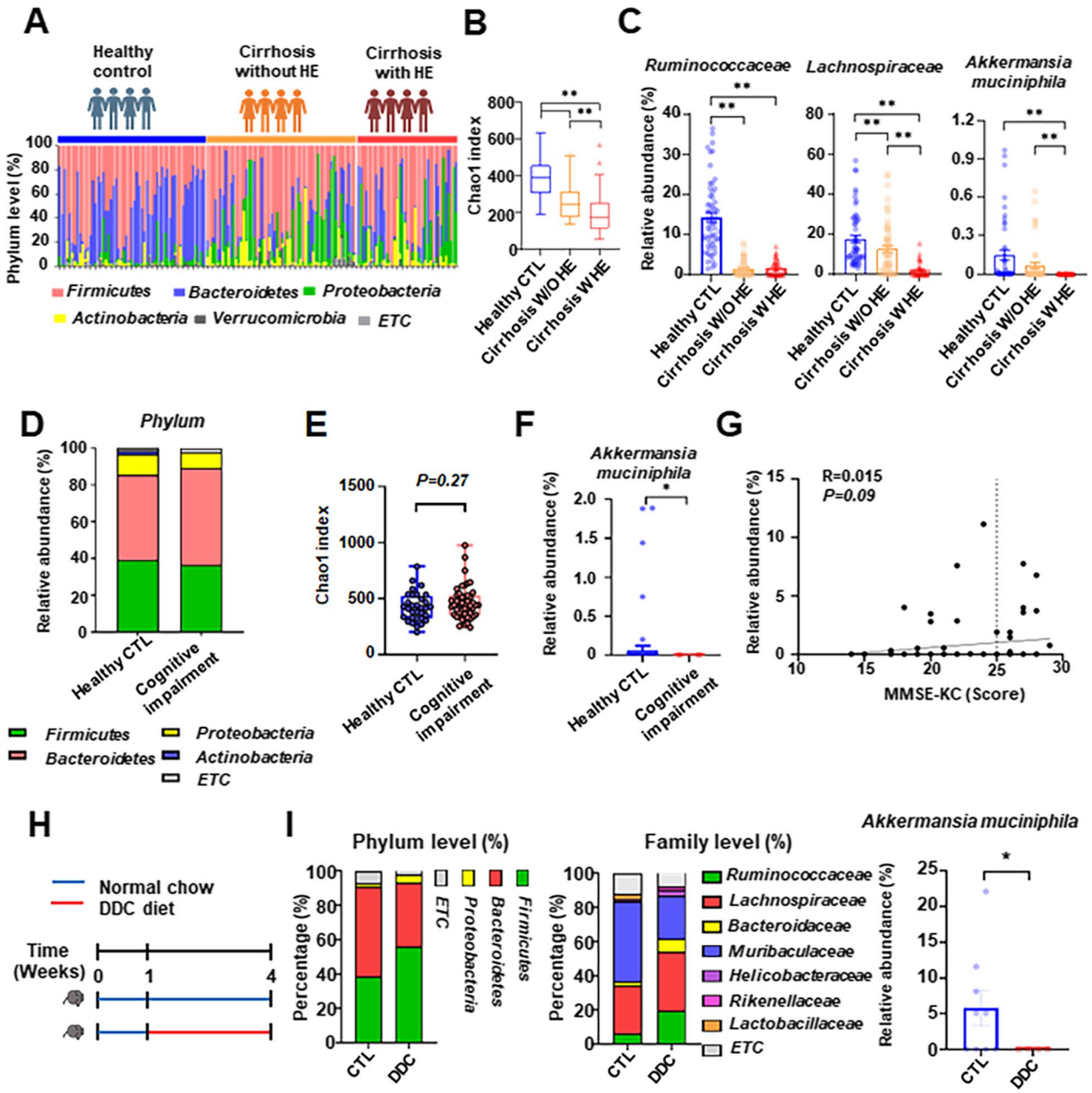

Fig. 1 Cirrhotic patients with hepatic encephalopathy and cognitive impairment patients exhibited a decreased fecal bacterial abundance of *Akkemansia muciniphila*, and which was also identified in animal models. **a** Taxa summary of bacterial phyla level obtained by 16S rDNA sequencing of fecal samples. **b** Microbial alpha diversity Chao1 in the context of disease progression classifications. $^{**}P < 0.01$; Wilcoxon rank-sum test. **c** Relative abundances of species with significantly different representations in human groups. Data represent the means ± SEM; $^{**}P < 0.01$; one-way ANOVA. **d** Relative abundance of bacterial phyla level obtained by 16S rDNA sequencing of fecal samples. **e** Microbial alpha diversity in patients with cognitive impairment. **f** Relative abundances of *A. muciniphila* in healthy control and cognitive impairment group. Data represent the means ± SEM; $^{*}P < 0.05$, unpaired t-test. **g** Pearson's correlation coefficients, *p* values, and linear relationships of *A. muciniphila* relative abundance (%) and MMSE-KC score. **h** Schematic of intervention with DDC diet (red) during the 3 weeks of 4 weeks DDC-induced liver injury animal model. **i** Relative abundance of phylum, family and *A. muciniphila* in control mice and DDC diet mice. AKK, *Akkermansia muciniphila*; AKKp, pasteurized *Akkermansia muciniphila*. Data represent the means ± SEM; n ≥ 3; $^{*}P < 0.05$; unpaired t-test

between groups, differences in *A. muciniphila* according to disease were commonly identified in both models (Supplementary Fig. 2).

To demonstrate the link between human liver disease phenomena and gut dysbiosis, we investigated animal models of liver disease in mice orally administered

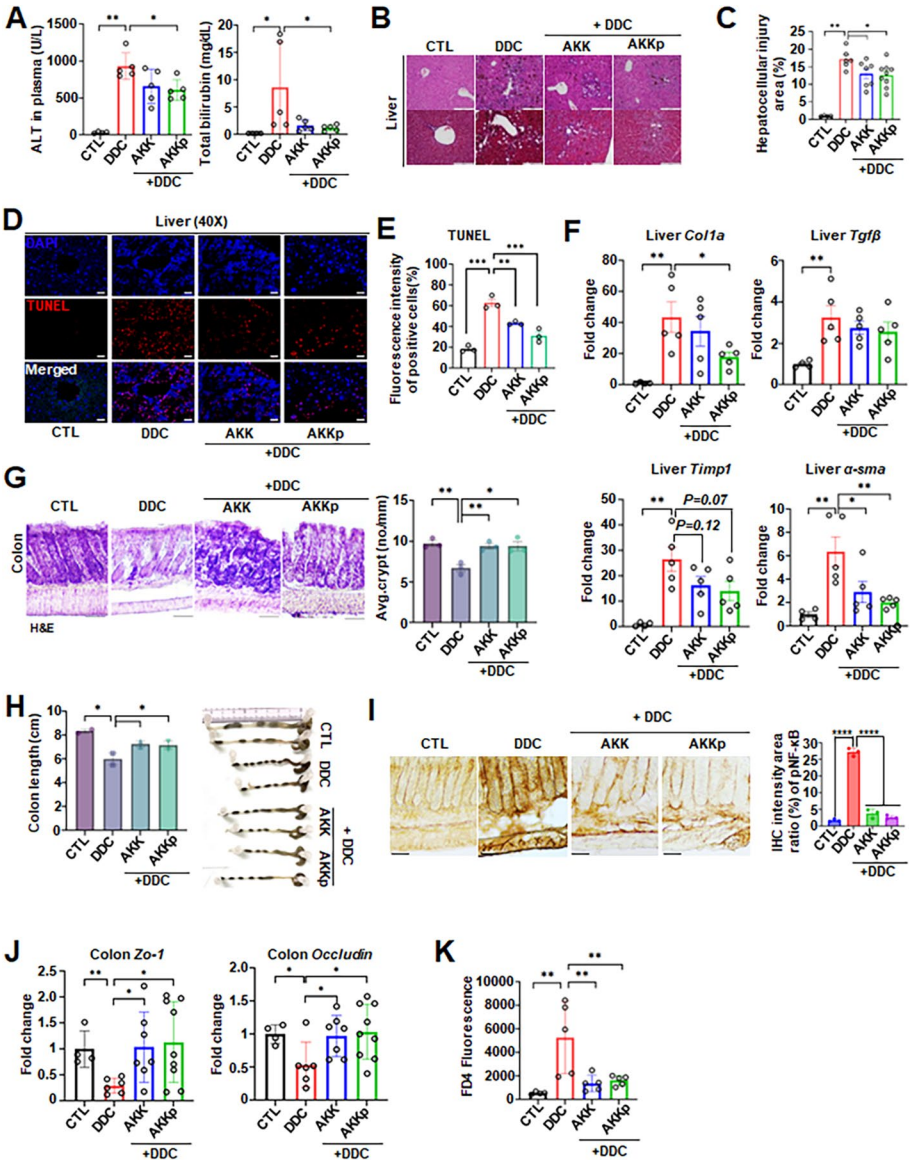

Fig. 2 Oral administration of *A. muciniphila* alleviates liver injury and protects intestinal barrier in a mouse model. **a** Plasma ALT and total bilirubin levels. Data represent the means ± SEM; $n \geq 4$; $^{**}P < 0.01$, $^{*}P < 0.05$; one-way ANOVA. **b**, **c** Histological assessment of liver injury with representative images of H&E and Masson's trichrome stained liver sections. Data represent the means ± SEM; $n \geq 3$; $^{**}P < 0.01$, $^{*}P < 0.05$; one-way ANOVA. Scale bar, 200 μm. **d**, **e** TUNEL staining in the liver from mouse. Data represent the means ± SEM; $n \geq 3$; $^{**}P < 0.01$ one-way ANOVA. Scale bar, 50 μm. **f** Hepatic mRNA expression of liver genes (*Col1a*, *Tgfβ*, *Timp1*, and *α-sma*). Data represent the means ± SEM; $n \geq 4$; $^{**}P < 0.01$, $^{*}P < 0.05$; one-way ANOVA. **g** Histological assessment of colon crypt with representative images of H&E stained colon sections. Data represent the means ± SEM; $n \geq 3$; $^{**}P < 0.01$, $^{*}P < 0.05$; one-way ANOVA. Scale bar, 200 μm. **h** GI tract dysfunction characterization measured by the colon length. Data represent the means ± SEM; $n = 3$; $^{*}P < 0.05$; one-way ANOVA. **i** Immunohistochemical staining of phosphorylated NFκB in the mouse colon. Data represent the means ± SEM; n ≥ 3; $^{****}P < 0.0001$ one-way ANOVA. Scale bar, 200 μm. **j** Colon mRNA expression of tight junction-related genes (*Zo-1*, *Occludin*). Data represent the means ± SEM; n ≥ 4; $^{**}P < 0.01$, $^{*}P < 0.05$; one-way ANOVA. **k** Plasma FD4 (fluorescein isothiocyanate dextran 4) level of the in vivo gut permeability assay. Data represent the means ± SEM; n ≥ 4; $^{**}P < 0.01$; one-way ANOVA

3,5-diethoxycarbonyl-1,4-dihydrocollidine (DDC) (Fig. 1H). A gut microbiome imbalance was observed at the phylum and family levels, and for specific species, the abundance of *A. muciniphila* decreased ($P=0.07$) with the progression of liver damage through the consumption of the DDC diet (Fig. 1I). These results indicate that the abundance of *A. muciniphila* in the gut is likely related to cognitive impairment and the progression of liver injury and may be an important factor. Interestingly, in an animal model of oral DDC administration that mimics human liver disease,

similar cirrhotic symptoms and cognitive impairment were observed. Furthermore, a histological evaluation of liver tissue using H&E staining revealed that hepatitis was significantly increased ($P=0.018$) in the DDC diet group. (Supplementary Fig. 3A and 3B). Notably, we detected neuronal cell death in the hippocampus associated with cognitive impairment in animal models of DDC-induced hepatocellular injury using IHC staining (Supplementary Fig. 3C and 3D). We detected damage to the enteric nerve layer with the PGP 9.5 antibody, which stains enteric neuronal cells (Supplementary Fig. 3E and 3F). Additionally, cognitive deficits due to hippocampal neuronal death were observed in the DDC diet group (Supplementary Fig. 3G). Through these results, we successfully established an animal model of liver disease and identified *A. muciniphila* depletion, consistent with the neuropsychiatric abnormalities observed in human patients.

Protective effects of *A. muciniphila* on gut inflammation and hepatocellular injury in a DDC diet animal model

We administered live or pasteurized *A. muciniphila* to C57BL/6 mice fed the DDC diets for 8 weeks to investigate the protective effect of A. muciniphila on liver damage, (Supplementary Fig. 4A). Afterward, we checked the plasma ALT and total bilirubin levels in the mice, which were consequently decreased in the DDC + *A. muciniphila*- and DDC + pasteurized *A. muciniphila*-treated groups compared to the DDC group (Fig. 2A). The effect of *A. muciniphila* on alleviating liver injury was confirmed by H&E and Masson's trichrome staining (Fig. 2B and C). Additionally, an increase in apoptosis in the DDC model was observed using TUNEL staining, confirming the effect of treatment with *A. muciniphila* or pasteurized *A. muciniphila* on decreasing apoptosis (Fig. 2D and E). The mRNA expression of liver genes (*Col1a1*, *Tgfβ*, *Timp1*, and α-*sma*) was also downregulated in both the DDC + *A. muciniphila*- and DDC + pasteurized *A. muciniphila*-treated groups compared to the DDC-only-treated group (Fig. 2F). The protective effect of *A. muciniphila* on enteric nerve layer damage was confirmed by H&E staining (Fig. 2G).

We also measured the shortening of the colon length, which is a measure of gut inflammation, and shortening symptoms were alleviated in both the DDC + *A. muciniphila*- and DDC + pasteurized *A. muciniphila*-treated groups (Fig. 2H). Additionally, the level of phosphorylated nuclear factor kappa B (pNF-kB) which is a hallmark of chronic inflammatory diseases, in the mouse colon was measured using IHC staining, and it was significantly reduced in both the DDC + *A. muciniphila*- and DDC + pasteurized *A. muciniphila*-treated groups (Fig. 2I). The mRNA expression of the proinflammatory cytokine *Tnfα* was downregulated in plasma. Additionally, a significant decrease ($P<0.05$) in the TNFα concentration was detected in liver tissue lysate samples. (Supplementary Fig. 4B).

We measured the mRNA expression levels of the tight junction proteins *Zo-1* and *Occludin* in mouse colon tissue to evaluate whether *A. muciniphila* prevents gut leakage. The results showed that the administration of DDC led to a decrease in the mRNA expression of the tight junction proteins *Zo-1* and *Occludin* in colonic tissue, which was restored by *A. muciniphila* administration (Fig. 2J). Fluorescein isothiocyanate-dextran 4 kDa (FD4) was applied to the intestinal mucosa and tracked systemically in the plasma to quantify gut leakiness, and *A. muciniphila* reduced the systemic translocation of FD4 (Fig. 2K). We also measured plasma lipopolysaccharide (LPS)/lipopolysaccharide-binding protein (LBP) concentrations and found that the administration of *A. muciniphila* reduced ($P \leq 0.05$) the plasma endotoxin concentrations (Supplementary Fig. 4C).

Furthermore, animal models of liver disease were created through bile duct ligation (BDL) surgery to determine the efficacy of *A. muciniphila* in various animal models of liver injury (Supplementary Fig. 5A). We administered *A. muciniphila* to the BDL surgery model, which causes hepatocellular injury and liver cell apoptosis, and it subsequently alleviated liver injury (Supplementary Fig. 5B). Similarly, the mRNA expression levels of liver genes (*Col1a1*, *Timp1*, and α-*sma*) were lower in mice administered *A. muciniphila* than in those in the BDL surgery-only group (Supplementary Fig. 5C). On the other hand, the mRNA expression level did not changed.

Reduction in gut inflammation and enteric neuronal cell death by *A. muciniphila* in a DDC diet animal model

We analyzed serotonin level in gut tissues through IHC staining using serotonin-specific antibodies to identify enteric neuronal cell death and gut inflammation in an animal model of liver disease generated by oral administration of DDC. We observed a significant decrease in 5-HT (5-hydroxytryptamine) expression in the enteric neuronal system (ENS) in the DDC-treated group compared to the control chow group. However, in the group treated with *A. muciniphila* and pasteurized *A. muciniphila*, we observed increased 5-HT expression. We also validated the improvement in gut leakage through structural analysis of colon tissue sections based on isolation of the enteric nerve layer (Fig. 3A and B). To assess whether DDC regulates Iba-1, PGP 9.5 (enteric neural marker) and 5-HT expression in the colon, we performed 5-HT/Iba-1 or Iba-1/PGP9.5 co-immunofluorescence staining. In the DDC treatment group, the amount of

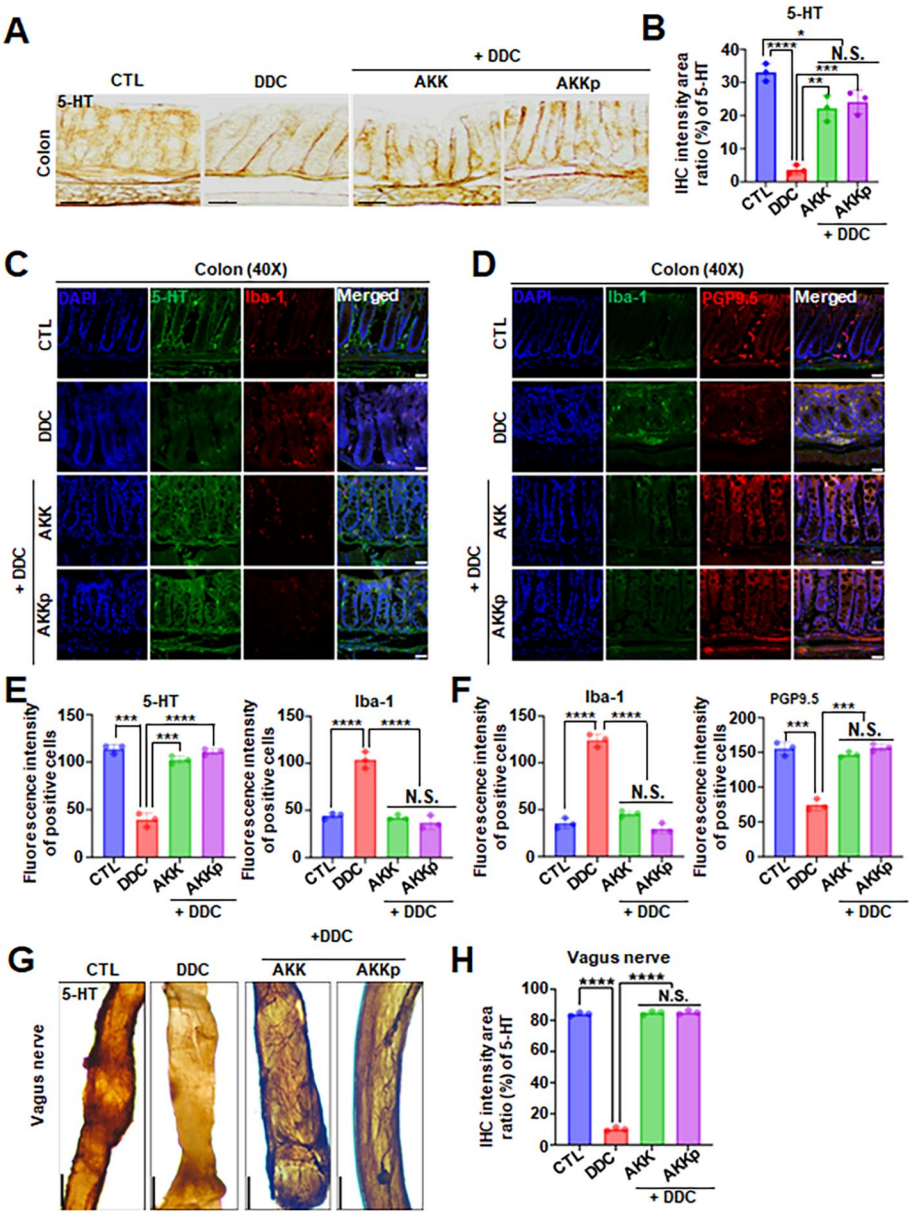

Fig. 3 Serotonin deficiency and activation of neuroinflammatory mechanisms in the gut and brain axis of a liver disease animal model and neuronal cell deaths alleviated by *A. muciniphila* administration. **a**, **b** Immunohistochemistry staining of 5-HT in the colon of mice. Quantitative analysis of 5-HT-positive cells. Data represent the means ± SEM; representative data of 3 samples; *****P* < 0.0001; N.S. = not significant, one-way ANOVA. Scale bar, 100 μm. **c** Immunofluorescent staining of anti-5-HT/anti-Iba-1 in the colon of mice and the fluorescent signals were quantified (**d**) Immunofluorescent staining of anti-Iba-1/anti-PGP9.5 in the colon of mice and the fluorescent signals were quantified (**e**) Scale bar, 10 μm. Data represent the means ± SEM; representative data of 3 samples; *****P* < 0.0001; N.S. = not significant, one-way ANOVA. **f** Scale bar, 10 μm. Data represent the means ± SEM; representative data of 3 samples; *****P* < 0.0001; N.S. = not significant, one-way ANOVA. **g**, **h** Therapeutic effect of AKK or pasteurized AKK (AKKp) treated groups in the vagus nerve of mice were analyzed by immunohistochemistry staining. Scale bar, 20 μm. Data represent the means ± SEM; representative data of 3 samples; *****P* < 0.0001; N.S. = not significant, one-way ANOVA

5-HT decreased and the expression of Iba-1 which indicates activated microglia increased compared that in the control group, but the inflammatory response was significantly improved in the group treated with *A. muciniphila* or pasteurized *A. muciniphila* in combination with DDC (Fig. 3C). The graph quantifying the results below the representative image confirms this finding (Fig. 3E). Furthermore, the increase in Iba-1 expression was accompanied by a decrease in PGP9.5 expression in the DDC-treated group, and an increase in PGP9.5

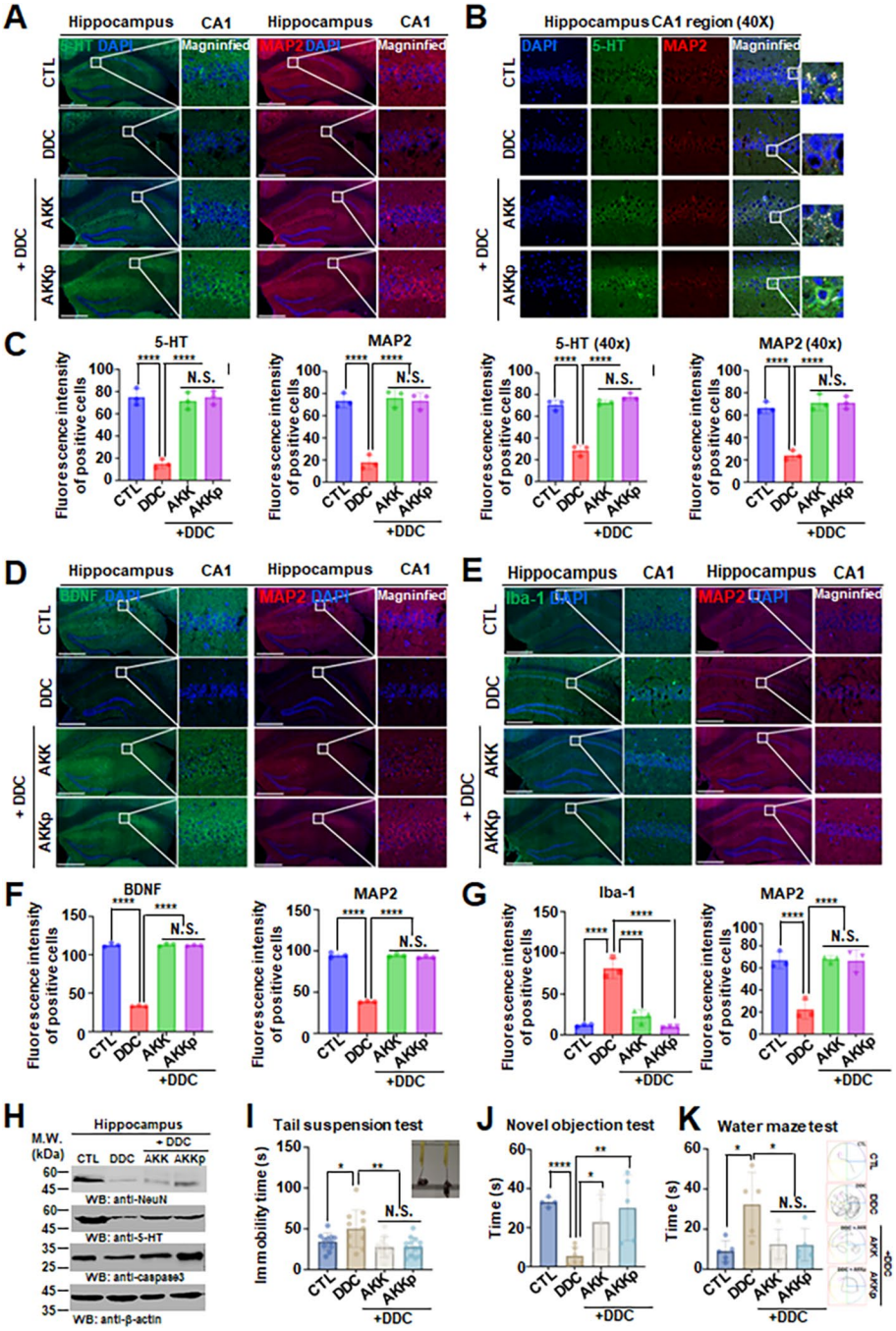

Fig. 4 Both BDNF and 5-HT are reduced in DDC only treated group hippocampus, while increased in *A. muciniphila* treated group. a, b, c Co-immunofluorescence staining analysis of anti-5-HT/anti-MAP2 in the hippocampus CA1 region of mice and the fluorescent signals (**a**, **b**) were quantified (**c**). Scale bar, 100 μm. Data represent the means ± SEM; representative data of 3 samples; ****$P < 0.0001$; N.S. = not significant, one-way ANOVA. **d**, **e**, **f**, **g** The immunofluorescence co-staining of anti-BDNF/anti-MAP2 (**d**, **f**) and anti-Iba-1/anti-MAP2 (**e**, **g**) in the hippocampus of the above animals. Scale bar, 100 μm. Data represent the means ± SEM; representative data of 3 samples; ****$P < 0.0001$; N.S. = not significant, one-way ANOVA. **h** Western blot analysis of prefrontal cortex and hippocampus lysates from the animals treated with DDC only or both treated DDC + AKK group or DDC + AKKp group. **i** Immobility time graph of tail suspension test. Data represent the means ± SEM; n ≥ 11; *$P < 0.05$, **$P < 0.01$; N.S. = not significant, unpaired t-test. **j** Cognitive impairment tests of novel objection test and water maze test (**k**) were performed. Data represent the means ± SEM; n ≥ 4; *$P < 0.05$, **$P < 0.01$; N.S. = not significant, unpaired t-test

expression was observed in the group treated with *A. muciniphila* or pasteurized *A. muciniphila*, confirming that *A. muciniphila* mitigated gut leakage and inflammation (Fig. 3D and F). Remarkably, immunohistochemical staining of the vagus nerve with a 5-HT-specific antibody revealed high 5-HT expression in the *A. muciniphila* and pasteurized *A. muciniphila* treatment groups. This result provides direct evidence that *A. muciniphila* specifically regulates expression in serotonergic interneurons (Fig. 3G and H).

Hippocampal neuronal cell death with cognitive impairment in an animal models of liver disease

We measured serotonin levels and the expression of the the neuronal marker microtubule associated protein-2 (MAP2) in the hippocampal brain region to determine the importance of the gut-liver-brain axis in animal models of liver disease. Surprisingly, the expression of serotonin and MAP2 was significantly reduced in the group receiving DDC orally compared to the control group. Furthermore, the DDC-induced decrease in serotonin and MAP2 expression were reversed in the group treated with *A. muciniphila* and pasteurized *A. muciniphila* (Fig. 4A, B, and C). Moreover, to determine whether *A. muciniphila* also affects dopamine expression, we examined dopamine expression in the substantia nigra of the brain and in the gut and vagus ganglia and found that dopamine expression was reduced by DDC but was not restored by *A. muciniphila* (Supplementary Fig. 6A, S6B, and S6C). The vagus nerve is a single neuron that connects the gut-brain axis and is referred to as the highway for neurotransmitters produced in the brain and gut [28, 29].

In addition, the levels of BDNF, a molecule that plays an important role in cognitive function in the brain, and Iba-1, a marker of activated microglia, were measured in each group. Similar to previous results, BDNF expression was reduced in the DDC-treated group (Fig. 4D), and Iba-1 expression was significantly increased (Fig. 4E). In contrast, quantitative and qualitative analyses confirmed that BDNF expression was increased and Iba-1 expression was decreased in DDC + *A. muciniphila*- or DDC + pasteurized *A. muciniphila*-treated groups (Fig. 4F and G). Similar observations were confirmed by immunoblotting. Increased neuronal death and 5-HT depletion was observed in the DDC-only group but the loss of hippocampal neurons and 5-HT was prevented in the DDC + *A. muciniphila*- or DDC + pasteurized *A. muciniphila*-treated groups (Fig. 4H). We also conducted animal behavioral experiments related to cognitive function and depression to determine the effects of neuronal death in the hippocampus and decreased expression of BDNF and serotonin and found that the DDC-treated group exhibited depression and cognitive dysfunction, which was improved in the *A. muciniphila* and pasteurized *A. muciniphila*-treated groups (Fig. 4I, J, and K). Additionally, the therapeutic effect of *A. muciniphila* was also confirmed in the BDL surgery model (Supplementary Fig. 6D and 6E). These scientific analyses suggest that the inflammatory mechanism and apoptosis of gut and brain neurons in animal models of liver disease may be regulated by *A. muciniphila*, which regulates BDNF and serotonin expression.

Sarpogrelate inactivates 5HT2A/2B receptors in liver tissue but does not affect the 5HT/5HT receptors in the gut or brain via the gut-organ *axis*

Sarpogrelate is a 5-HT2A and 2B receptor antagonist that has been shown to inhibit the action of serotonin in the body. In the liver, serotonin is synthesized and released by platelets and contributes to the development of liver injury and portal hypertension in patients with cirrhosis [30, 31]. To investigate the inflammatory mechanisms and cognitive dysfunction of brain serotonergic neurons ameliorated by increased serotonin secretion by *A. muciniphila* in combination with sarpogrelate, we treated the animal model of DDC-induced liver injury with sarpogrelate for 5 weeks (Supplementary Fig. 7A). Consequently, the effect of sarpogrelate on alleviating liver injury was confirmed by H&E staining (Supplementary Fig. 7B), and the mRNA expression of liver genes (*Col1a*, *Tgfβ*, *Timp1*, and *α-sma*) was also downregulated in the DDC + sarpogrelate + *A. muciniphila*- or DDC + sarpogrelate + pasteurized *A. muciniphila*-treated groups compared to the group treated without sarpogrelate (Supplementary Fig. 7C). However, we found that sarpogrelate had no effect on the inflammatory mechanisms and cognitive dysfunction, or serotonergic neurons in the brain (Supplementary Fig. 8). These results suggest the existence of a vagus ganglion-mediated gut-brain axis connection and a survival mechanism for serotonergic neurons in the hippocampal region of the brain that is mediated solely by nonblood neurotransmitters.

The administration of *A. muciniphila* alleviates liver injury by suppressing 5-HT2A/2B receptor expression

To investigate whether *A. muciniphila* relieves liver injury through serotonin receptors, we measured 5-HTR2A/2B expression levels in mouse liver tissue (Fig. 5A, C, E, and G). The expression of 5-HTR2A/2B was significantly increased in the group orally administered DDC compared to the control group. In addition, the increase in 5-HTR2A/2B expression induced by DDC was reduced in the groups treated with *A. muciniphila* and pasteurized *A. muciniphila*. The expression of the receptors was examined in the liver tissue of a hepatocellular injury

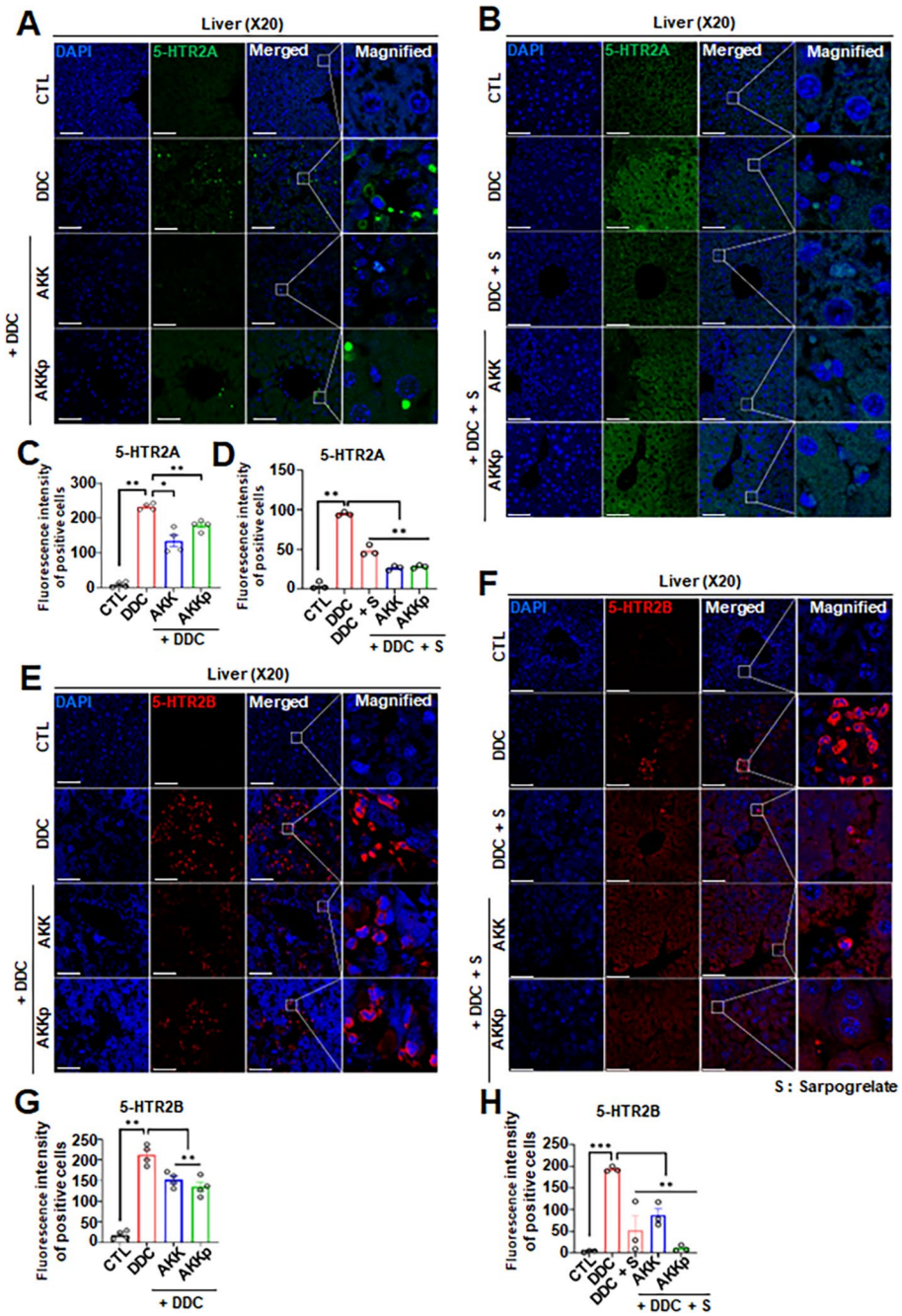

Fig. 5 5-HT2A/2B receptor expression are increased in DDC only treated group liver tissue, while reduced in *A. muciniphila* treated group. **a**, **b**, **c**, **d** immunofluorescence staining analysis of anti-5-HTR2A in the liver tissue of mice and the fluorescent signals (**a**, **b**) were quantified (**c**, **d**). Scale bar, 100 μm. Data represent the means ± SEM; n ≥ 3; $^{**}P < 0.01$, $^{*}P < 0.05$; one-way ANOVA. **e**, **f**, **g**, **h** immunofluorescence staining analysis of anti-5-HTR2B in the liver tissue of the above mice. The fluorescent signals (**e**, **f**) were quantified (**g**, **h**). Scale bar, 100 μm. Data represent the means ± SEM; n ≥ 3; $^{***}P < 0.005$, $^{**}P < 0.01$; one-way ANOVA

mouse model treated with sarpogrelate to determine whether the 5-HTR2A/2B antagonist has an effect on *A. muciniphila*-induced expression reduction, (Fig. 5B, D, F, and H). Additionally, we confirmed whether 5-HTR2A/2B expression levels change in cell experiments. When the LX-2 human hepatic stellate cell line was treated with sarpogrelate or pasteurized *A. muciniphila*, the expression levels of 5-HTR2A/2B decreased,

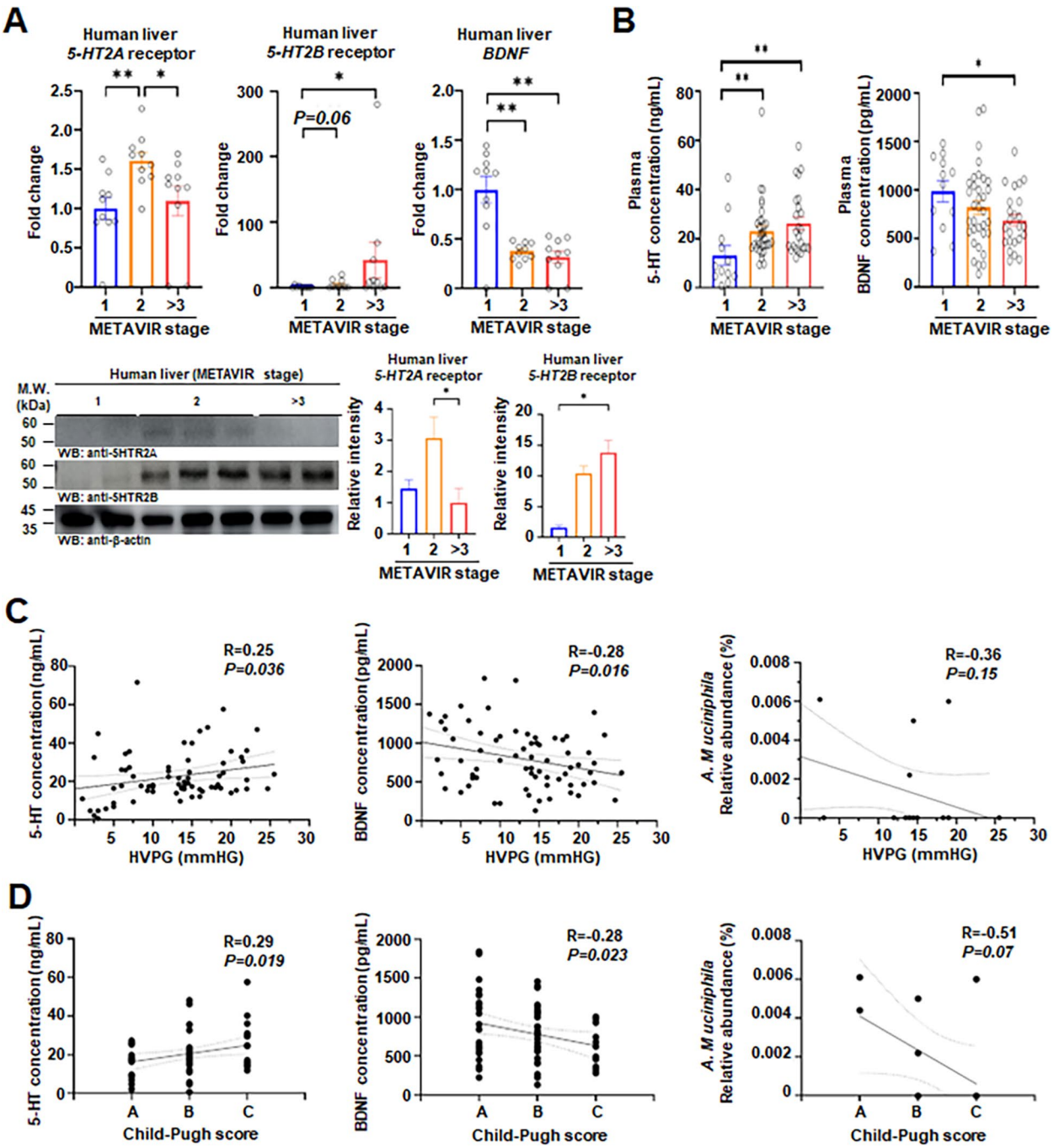

Fig. 6 BDNF/serotonin is associated with the progression of liver cirrhosis. **a** mRNA expression of 5-HT2A receptor and 5-HT2B receptor, and BDNF in human liver biopsy. Western blot analysis of 5-HT2A receptor and 5-HTR2B receptor in human liver biopsy. Data represent the means ± SEM; $n = 10$; $^{**}P < 0.01$, $^{*}P < 0.05$. one-way ANOVA. **b** Concentrations of serotonin and BDNF measured in portal blood of patients with liver cirrhosis. Data represent the means ± SEM; n ≥ 12; $^{**}P < 0.01$, $^{*}P < 0.05$. one-way ANOVA. **c** Pearson's correlation coefficients, *P* values, and linear relationships of serotonin and BDNF concentration, *A. muciniphila* relative abundance, and HVPG. **d** Pearson's correlation coefficients, *p* values, and linear relationships of serotonin and BDNF concentration, A. muciniphila relative abundance, and Child–Pugh score

which was consistent with the results from the animal model (Supplementary Fig. 7D). Taken together, these results suggest that administration of *A. muciniphila* or pasteurized *A. muciniphila* can achieve the remission of liver injury by inhibiting 5-HTR2A/2B, which contributes to liver injury activity by binding to serotonin.

Validation of the correlation between BDNF/serotonin levels and disease progression in human subjects with liver fibrosis and cirrhosis

Since *A. muciniphila* had a positive effect on the gut-liver-brain axis through the regulation of serotonin and the recovery of BDNF levels in the brain, gut and liver in the animal model of liver injury, we checked plasma serotonin levels in the animal model, which were markedly reduced by DDC and recovered by *A. muciniphila* (Supplementary Fig. 9A). Additionally, the expression of 5-HT2A/2B mRNA in mouse liver tissue was confirmed (Supplementary Fig. 9B). No significant difference was observed in 5-HT2A receptor expression, but the 5-HT2B receptor expression level was significantly decreased by pasteurized *A. muciniphila*.

We verified the changes in serotonin and BDNF according to the exacerbation of liver cirrhosis by analyzing portal blood and liver biopsies from human subjects (Fig. 6). Biopsy samples from patients with liver disease confirmed the mRNA expression of the 5-HT2A/2B receptor and BDNF (Fig. 6A). The expression of the 5-HT2A receptor was increased in patients with stage 2 hepatitis compared with patients with fatty liver disease (stage 1). However, a reduction was observed in stage 3 patients or patients with advanced fibrosis (cirrhosis). In contrast, the 5-HT2B receptor was activated and its levels were significantly increased in stage 3 patients and patients with severe cirrhosis. Similar observations were confirmed by immunoblotting. 5-HT2A receptor expression increased from stage 1 to stage 2 and decreased in stage 3. Additionally, 5-HT2B receptor expression increased as the stage progressed (Fig. 6A). We found that BDNF steadily decreases with the progression of liver disease, a pattern that was consistent with findings from patient with liver disease and various animal models of liver disease (Fig. 6B). The hepatic portal blood we sampled was associated with portal hypertension, a common symptom in patients with hepatopathy, which allowed us to specifically identify the increase in serotonin associated with increased blood cells [32].

We confirmed the correlation between HVPG, serotonin, BDNF, and *A. muciniphila* abundance and validated the association with liver cirrhosis (Fig. 6C). A positive correlation was observed between serotonin concentrations and HVPG, whereas a negative correlation was observed with BDNF concentrations. In addition, a negative correlation was observed between the HVPG and the relative abundance of *A. muciniphila*, which was confirmed to have a positive effect on the liver and cognitive function in animal models. These results were the same even when the patient group was divided based on Child–Pugh score (Fig. 6D). Hence, the current results suggest that BDNF is another important molecule in addition to serotonin in human liver disease progression and cirrhosis.

Discussion

We observed a decrease in the abundance of *Lachnospiraceae* and *Ruminococcaceae* and a change in alpha diversity in the gut microbiota of patients with liver cirrhosis, as previously reported, but no significant change was observed in the gut microbiome of subjects with simple cognitive impairment. Interestingly, we found a common *A. muciniphila* depletion in subjects with cirrhosis and cognitive impairment. Several studies have reported preventive and protective effects against cognitive impairment occurring in neuropsychiatric disorders through supplementation with *A. muciniphila* [33, 34]. Cognitive dysfunction caused by hepatic encephalopathy, a major complication of liver cirrhosis, is manifested by the disruption of the gut-liver-brain axis, and we hypothesized that *A. muciniphila* depletion is strongly correlated with liver disease and cognitive function [35].

Prior to validation in animal models, a plan to induce liver disease by administering a DDC diet was established and evaluated to mimic the state of cognitive impairment caused by liver injury. Considering the effect on the gut microflora, liver damage was induced by diet rather than drugs, and the occurrence of disorders in the gut-liver-brain axis and a decrease in the abundance of *A. muciniphila* were confirmed to indicate its suitability for use as an animal model. In several studies, the evaluation and efficacy of *A. muciniphila* in treating metabolic diseases and diabetes were verified, and the effect of pasteurization was confirmed [36, 37]. Pasteurization can be effective in the host, as it can increase the accessibility of certain bacterial compounds that have a positive effect. Interestingly, in the animal experiments, the hepatocyte injury induced by biliary injury was effectively inhibited by pasteurized *A. muciniphila* treatment. Surprisingly, serotonin (5-HT), which is associated with cognitive function, was detected in the enteric plexus and vagus nerve in a mouse model of DDC-induced hepatocellular injury. Although several other neurotransmitters were also depleted, serotonin was the only neurotransmitter whose levels were restored by reintroduction of *A. muciniphila.* The mechanism by which 90% of the serotonin delivered to the brain is produced by enteric neurons and transmitted to the brain via the vagus nerve indicates that the liver, gut, and brain actively interact through neurotransmitter and neurohormone secretion from the vagus nerve. The same effect was observed on the animal model of BDL surgery-induced liver injury.

In particular, the reduction in *Tnfα* levels in plasma was greater after treatment with pasteurized *A. muciniphila*,

suggesting that inflammation caused by the bacterial compounds was reduced. Further investigation of the detailed molecular mechanism by which pasteurization and pasteurization-produced bacterial compounds alleviate liver injury is necessary.

Previous studies have shown that serotonin and serotonin receptor signaling are correlated with liver disease [38]. Hepatic steatosis can be improved by reducing hepatic 5-HTR2A signaling [39]. Additionally, 5-HTR2B stimulation of activated hepatic stellate cells plays an important role in directing the balance between cell regeneration and fibrosis, and antagonism of 5-HTR2B attenuates fibrosis [40]. Overall, the serotonin signaling system in the liver plays an important role in liver injury and cell regeneration and consequently its modulation can be used as a therapeutic approach [41]. However, the mode of action of this serotonin signaling system and the identification of regulatory factors need further confirmation in the future.

We verified that the administration of *A. muciniphila* could act as one of these modulators. *A. muciniphila* antagonized the expression of 5-HTR2A/2B in the liver and alleviated liver injury. Liver tissue mRNA expression did not reflect the exact expression, but histological evaluation through immunofluorescence staining confirmed a tendency for the expression of these receptors to decrease.

Moreover, in liver biopsies collected from patients with liver disease, 5-HTR2A expression was elevated in patients with hepatitis and decreased in patients with cirrhosis. Considering that 5-HTR2A contributes to hepatic steatosis, we confirmed that 5-HTR2A is activated until the hepatitis stage, after which its activity decreases as the liver enters cirrhosis, and then fibrosis is activated through the increased expression of 5-HTR2B. Consistent with the expression of serotonin receptors, serotonin levels in the portal vein increases with the progression of cirrhosis. The importance of serotonin in the pathogenesis of portal hypertension has been highlighted in previous studies and is strongly linked to reversible portal systemic encephalopathy [42, 43]. In addition, we confirmed that the level of the BDNF molecule, which is linked to the cognitive impairment commonly found in cirrhotic patients, was significantly reduced in patients with cirrhosis and hepatitis.

Regarding the causal relationship between brain cognitive impairment induced by liver injury and *A. muciniphila*, to date, no study has shown this causal association with strong evidence. Few reports have indirectly proven the relationship between brain cognitive impairment induced by liver injury and *A. muciniphila* [12, 44]. In patients with sarcopenic cirrhosis, a decreased proportion of *A. muciniphila* is correlated with unfavorable outcomes [45]. In addition, *A. muciniphila* was associated with decreased neuroinflammation in mice colonized after fecal microbiota transplantation from humans with cirrhosis [46]. Similarly, *Verrucomicrobiaceae*, to which *A. muciniphila* belongs, was correlated with cognitive improvement and reduced inflammation after fecal microbiota transplantation [47]. In our study, we showed for the first time the therapeutic effect of *A. muciniphila* on cognitive dysfunction and liver fibrosis and verified this effect through animal experiments and analyses of human tissue.

Microbiota-derived metabolites have been reported to be key regulators of various diseases [48]. *A. muciniphila* is also associated with disease control through metabolites [49]. In our study, administration of *A. muciniphila* recovered the levels of proinflammatory cytokines, endotoxin (LPS and LBP), serotonin associated cognitive function, and liver injury, suggesting that *A. muciniphila* acts as a cornerstone in regulating the gut-liver-brain axis.

Furthermore, after oral administration of *A. muciniphila* to an animal model of liver injury, RNA analysis of liver tissue revealed increased expression of various molecules that play important roles in neuroplasticity, with BDNF identified as the key molecule. This protein is an overlapping molecule that has been identified in patients with hepatic encephalopathy and is associated with liver disease in humans and animals. Taken together, the identification of the regulation of the serotonin and BDNF molecules by *A. muciniphila* suggests novel molecular pharmacology for identifying the mechanisms of microbial therapy. Overall, we suggest that *A. muciniphila* may be beneficial for patients with liver disease and cognitive impairment.

Abbreviations

A. muciniphila	*Akkermansia muciniphila*
BDNF	Brain-derived neurotrophic factor
LPS	Lipopolysaccharide
LBP	Lipopolysaccharide-binding protein
BDL	Bile duct ligation
HVPG	Hepatic venous pressure gradient
HE	Hepatic encephalopathy
ENS	Enteric neuronal system
ALT	Alanine aminotransferase
AST	Aspartate aminotransferase
GGT	Gamma-glutamyl transferase
5-HT	5-Hydroxytryptamine
DDC	3,5-Diethoxycarbonyl-1,4-dihydrocollidine
TH	Tyrosine hydroxylase
MAP2	Microtubule associated protein-2

Supplementary Information

The online version contains supplementary material available at https://doi.org/10.1186/s40168-024-01924-8.

Supplementary Material 1: Supplementary Fig. 1. Gut microbiota family level and alpha diversity in cirrhotic patients and cognitive impairment

patients. (a) Plasma ALT and AST levels in human groups. Data represent the means ± SEM; $^{**}P < 0.01$, $^{*}P < 0.05$; one-way ANOVA. (b) Relative abundance of bacterial family level obtained by 16S rDNA sequencing of cirrhotic patients fecal samples. (c) Microbial alpha diversity (ACE and Shannon) in cirrhotic patients fecal samples. $^{*}P < 0.05$, $^{**}P < 0.01$; Wilcoxon rank-sum test. (d) Relative abundance of bacterial family level obtained by 16S rDNA sequencing of cognitive impairment patients fecal samples. (e) Microbial alpha diversity Shannon in cognitive impairment patients fecal samples. Wilcoxon rank-sum test. Supplementary Fig. 2. Linear discriminant effect size analysis results in cirrhotic patients and cognitive impairment patients. (a) Histogram of the linear discriminant analysis (LDA) scores and taxonomic representation differentially abundant in cirrhotic patients without HE, cirrhotic patients with HE and healthy subjects. (b) Histogram of the LDA scores and taxonomic representation differentially abundant in cognitive impairment patients and healthy subjects. Supplementary Fig. 3. Gut-liver-brain axis damage and cognitive decline in a liver disease mouse model. (a, b) Histological assessment of liver injury with representative images of H&E and Masson's trichrome stained liver sections. Data represent the means ± SEM; n ≥ 3; $^{*}P < 0.05$, unpaired t-test. Scale bar, 200 μm. (c, d) Representative images of immunohistochemistry staining of TH in the hippocampus region of mice and quantitative analysis of TH-positive cells. Data represent the means ± SEM; representative data of 3 samples;$^{****}P < 0.0001$; unpaired t-test. Scale bar, 200 μm (e, f) Representative images of immunohistochemistry staining of TH in the colon region of mice and quantitative analysis of TH-positive cells. Data represent the means ± SEM; representative data of 3 samples; $^{****}P < 0.0001$; unpaired t-test. Scale bar, 100 μm (g) Cognitive impairment tests of novel objection test and t-maze test were performed. Data represent the means ± SEM; n ≥ 6; $^{**}P < 0.01$; N.S. = not significant, unpaired t-test. Supplementary Fig. 4. Effects of *A. muciniphila* on *Tnfα* and gut permeability in the DDC mouse model. (a) Schematic of study design. Mice was intervention with antibiotics or vehicle control during the 4 weeks. And then, mice were placed on normal chow or DDC diet for 8 weeks with oral *A. muciniphila* (live or pasteurization) administration. (b) Hepatic mRNA expression of *Tnfα*. TNFα concentrations in liver tissue and plasma a CBA kit was used to measure the levels of cytokines. Data represent the means ± SEM; n ≥ 4; $^{*}P < 0.05$, $^{**}P < 0.01$; one-way ANOVA. (c) Plasma lipopolysaccharide and lipopolysaccharide-binding protein concentrations in the DDC mouse model. Data represent the means ± SEM; n ≥ 4; $^{*}P < 0.05$; one-way ANOVA. Supplementary Fig. 5. Oral *A. muciniphila* administration alleviates liver damage in BDL mouse model. (a) Schematic of study design. Mice underwent bile duct ligation surgery, and after 5 days of recovery, pasteurized *A. muciniphila* was orally administered. (b) Histological assessment of liver injury with representative images of H&E and Masson's trichrome stained liver sections (c) Hepatic mRNA expression of liver genes (*Col1a, Tgfβ, Timp1*,and *α-sma*). Data represent the means ± SEM; n = 3; $^{**}P < 0.01$, $^{*}P < 0.05$; one-way ANOVA. Supplementary Fig. 6. *A. muciniphila* induces dopaminergic neuronal loss and motor dysfunctions in mice while restores serotonergic neurons in BDL surgery mice model. (a) Representative images of immunohistochemistry staining of TH in the SN region (upper), colon (middle) and vagus nerve (bottom) of mice and quantitative analysis of TH-positive cells (b). Data represent the means ± SEM; representative data of 3 samples; $^{****}P < 0.0001$; one-way ANOVA. Scale bar, 200 μm (upper), 100 μm (middle) and 50 μm (bottom). (c) Motor behavioral assay of nest building tests were performed. Data represent the means ± SEM; n ≥ 4; $^{*}P < 0.05$, $^{**}P < 0.01$; N.S. = not significant, unpaired t-test. (d) NeuN, 5-HT and Iba-1 staining in mouse hippocampus region by immunohistochemistry. Scale bar, 100 μm (e) Data represent the means ± SEM; representative data of 3 samples; $^{****}P < 0.0001$; one-way ANOVA. Supplementary Fig. 7. Sarpogrelate treatment enhances alleviation of liver injury by *A. muciniphila* in chronic hepatocellular injury mice model. (a) Schematic of study design. Mice was intervention with antibiotics or vehicle control during the 1 weeks. And then, mice were placed on normal chow or DDC diet for 3 weeks with oral *A. muciniphila* (live or pasteurization) and sarpogrelate (30 mg/kg) administration. (b) Histological assessment of hepatocyte injury with representative images of H&E stained liver sections. Scale bar, 200 μm. (c) Hepatic mRNA expression of liver genes (*Col1a, Tgfβ, Timp1*,and*α-sma*). Data represent the means ± SEM; n = 5; $^{**}P < 0.01$, $^{*}P < 0.05$ compared to DDC group. $^{\#\#}P < 0.01$, $^{\#}P < 0.05$ compared to sarpogrelate treated group; one-way ANOVA. (d) mRNA expression of 5-HT2A receptor and 5-HT2B receptor in LX-2 cells. Data represent the means ± SEM; $n = 4$; $^{*}P < 0.05$; one-way ANOVA. Supplementary Fig. 8. Sarpogrelate blocks the restorative effect of *A. muciniphila*in chronic hepatocellular injury mice model. (a, b, c, d, e, f) Immunofluorescent staining of anti-5-HT/anti-MAP2 (a), anti-BDNF/anti-MAP2 (c) and anti-Iba-1/anti-MAP2 (e) in the hippocampus of mice and fluorescent signals were quantified (b, d, f). Data represent the means ± SEM; representative data of 3 samples;$^{****}P < 0.0001$; N.S. = not significant, unpaired t-test. Scale bar, 100 μm. Supplementary Fig. 9. Plasma serotonin concentration and liver tissue 5-HT2A/2B receptor mRNA expression levels in DDC mouse model. (a) Concentrations of serotonin measured in cardiac and portal vein blood. Data represent the means ± SEM; n ≥ 3; $^{**}P < 0.01$, $^{*}P < 0.05$; one-way ANOVA. (b) mRNA expression of *5-ht2a* receptor and *5-ht2b* receptor in mouse liver. Data represent the means ± SEM; $n = 5$; $^{**}P < 0.01$, $^{*}P < 0.05$; N.S. = not significant, one-way ANOVA.

Authors' contributions

K.T.S., E.H.A., and S.M.W. developed the rationale and designed the experiments, analyzed the data, and wrote the manuscript. E.J.K., M.G.C., and G.H.K. performed most of the experiments and data analysis. E.H.A. and E.J.K. performed studies on animal behavior experiments and brain-gut axis data analysis. M.G.C., G.H.K., S.H.H. and S.J.Y. provided technical assistance and liver-brain axis data analysis. S.K.L., M.E.A., and K.T.S. assisted with human patient data analysis and interpretation with critical human patient sample handling.

Funding

This research was supported by the National Research Foundation of Korea (NRF) grant funded by the Korea government (MSIT) (No. 2022R1C1C1006166) and Hallym University Research Fund, 2021 (HRF-202103-009) to E.H.A. This research was supported by Hallym University Research Fund, the Basic Science Research Program through the NRF funded by the Ministry of Education, Science and Technology (NRF-2020R1A6A1A03043026), Korea Institute for Advancement of Technology (P0020622).

Availability of data and materials

The authors declare that all data supporting the findings of this study are available within the article and its Supplementary information files or from the corresponding author upon request.

Declarations

Ethics approval and consent to participate

The study protocols conformed to the ethical guidelines of the 1975 Declaration of Helsinki as reflected in the a priori approval by the institutional review board for human research of all participating hospitals. Informed consent for participation in the study was obtained from each patient.

Consent for publication

Not applicable.

Competing interests

The authors declare no competing interests.

Author details

[1]Department of Physiology, College of Medicine, Hallym University, Hallymdaehak-Gil 1, Chuncheon-Si, Gangwon-Do 24252, South Korea. [2]Institute for Liver and Digestive Diseases, Hallym University College of Medicine, Chuncheon-Si, Gangwon-Do 24253, South Korea. [3]Department of Pathology, College of Medicine, Hallym University, Hallymdaehak-Gil 1, Chuncheon-Si, Gangwon-Do 24252, South Korea. [4]Department of Psychiatry, Chuncheon Sacred Heart Hospital, Hallym University College of Medicine, Chuncheon-si, Gangwon-Do, 24253 Chuncheon-Si, South Korea. [5]Department of Emergency Medicine, Hallym University, Chuncheon Sacred Heart Hospital, Chuncheon-Si, Gangwon-Do 24253, South Korea. [6]Department of Neurology, College of Medicine, Hallym University, Hallymdaehak-Gil 1, Chuncheon-Si, Gangwon-Do 24252, South Korea.

Received: 29 October 2023 Accepted: 2 September 2024
Published online: 28 September 2024

References

1. Butterworth RF. Hepatic Encephalopathy in Cirrhosis: Pathology and Pathophysiology. Drugs. 2019;79(Suppl 1):17–21.
2. Shawcross DL, Thabut D, Amodio P. Ammonia - an enduring foe - What evaluating whole body ammonia metabolism can teach us about cirrhosis and therapies treating hepatic encephalopathy. J Hepatol. 2023;79(2):266–8.
3. Korean Association for the Study of the L. KASL clinical practice guidelines for liver cirrhosis: Varices, hepatic encephalopathy, and related complications. Clin Mol Hepatol. 2020;26(2):83–127.
4. Haeussinger D, Dhiman RK, Felipo V, Görg B, Jalan R, Kircheis G, et al. Hepatic encephalopathy Nature Reviews Disease Primers. 2022;8(1):43.
5. Tonon M, Piano S. Acute on chronic liver failure in cirrhosis. Clin Mol Hepatol. 2022;28(2):273–5.
6. Davis BC, Bajaj JS. Effects of Alcohol on the Brain in Cirrhosis: Beyond Hepatic Encephalopathy. Alcohol Clin Exp Res. 2018;42(4):660–7.
7. Bass NM, Mullen KD, Sanyal A, Poordad F, Neff G, Leevy CB, et al. Rifaximin treatment in hepatic encephalopathy. N Engl J Med. 2010;362(12):1071–81.
8. Derrien M, Vaughan EE, Plugge CM, de Vos WM. Akkermansia muciniphila gen. nov., sp. nov., a human intestinal mucin-degrading bacterium. Int J Syst Evol Microbiol. 2004;54(5):1469–76.
9. Collado MC, Derrien M, Isolauri E, de Vos WM, Salminen S. Intestinal integrity and Akkermansia muciniphila, a mucin-degrading member of the intestinal microbiota present in infants, adults, and the elderly. Appl Environ Microbiol. 2007;73(23):7767–70.
10. Png CW, Linden SK, Gilshenan KS, Zoetendal EG, McSweeney CS, Sly LI, et al. Mucolytic bacteria with increased prevalence in IBD mucosa augment in vitro utilization of mucin by other bacteria. Am J Gastroenterol. 2010;105(11):2420–8.
11. Park JW, Suk KT. The effect of moderate alcohol consumption on nonalcoholic fatty liver disease. Clin Mol Hepatol. 2023;29(2):408–10.
12. Grander C, Adolph TE, Wieser V, Lowe P, Wrzosek L, Gyongyosi B, et al. Recovery of ethanol-induced Akkermansia muciniphila depletion ameliorates alcoholic liver disease. Gut. 2018;67(5):891–901.
13. Depommier C, Everard A, Druart C, Plovier H, Van Hul M, Vieira-Silva S, et al. Supplementation with Akkermansia muciniphila in overweight and obese human volunteers: a proof-of-concept exploratory study. Nat Med. 2019;25(7):1096–103.
14. Yaghoubfar R, Behrouzi A, Ashrafian F, Shahryari A, Moradi HR, Choopani S, et al. Modulation of serotonin signaling/metabolism by Akkermansia muciniphila and its extracellular vesicles through the gut-brain axis in mice. Sci Rep. 2020;10(1):22119.
15. Yaghoubfar R, Behrouzi A, Zare Banadkoki E, Ashrafian F, Lari A, Vaziri F, et al. Effect of Akkermansia muciniphila, Faecalibacterium prausnitzii, and Their Extracellular Vesicles on the Serotonin System in Intestinal Epithelial Cells. Probiotics Antimicrob Proteins. 2021;13(6):1546–56.
16. Sartor RB. Mechanisms of disease: pathogenesis of Crohn's disease and ulcerative colitis. Nat Clin Pract Gastroenterol Hepatol. 2006;3(7):390–407.
17. Angelucci F, Spalletta G, di Iulio F, Ciaramella A, Salani F, Colantoni L, et al. Alzheimer's disease (AD) and Mild Cognitive Impairment (MCI) patients are characterized by increased BDNF serum levels. Curr Alzheimer Res. 2010;7(1):15–20.
18. Ahn EH, Kang SS, Liu X, Cao X, Choi SY, Musazzi L, et al. BDNF and Netrin-1 repression by C/EBPbeta in the gut triggers Parkinson's disease pathologies, associated with constipation and motor dysfunctions. Prog Neurobiol. 2021;198: 101905.
19. Friswell M, Campbell B, Rhodes J. The role of bacteria in the pathogenesis of inflammatory bowel disease. Gut and liver. 2010;4(3):295.
20. Cohen C, Kodas E, Griebel G. CB1 receptor antagonists for the treatment of nicotine addiction. Pharmacol Biochem Behav. 2005;81(2):387–95.
21. Butterworth RF. Pathophysiology of hepatic encephalopathy: a new look at ammonia. Metab Brain Dis. 2002;17(4):221–7.
22. Ramachandran V, Ding B, George R, Novakovic M. Conservative management of severe serotonin syndrome with coma, myoclonus, and crossed-extensor reflex complicated by hepatic encephalopathy. Proc (Bayl Univ Med Cent). 2018;31(1):112–4.
23. Bosch J, Abraldes JG, Berzigotti A, Garcia-Pagan JC. The clinical use of HVPG measurements in chronic liver disease. Nat Rev Gastroenterol Hepatol. 2009;6(10):573–82.
24. Garcia-Tsao G. Can We Rely on Changes in HVPG in Patients with Cirrhosis? Hepatology. 2021;74(6):2945–7.
25. Zarrinpar A, Chaix A, Xu ZZ, Chang MW, Marotz CA, Saghatelian A, et al. Antibiotic-induced microbiome depletion alters metabolic homeostasis by affecting gut signaling and colonic metabolism. Nat Commun. 2018;9(1):2872.
26. Edgar RC. Search and clustering orders of magnitude faster than BLAST. Bioinformatics. 2010;26(19):2460–1.
27. Xie JT, Shao ZH, Vanden Hoek TL, Chang WT, Li J, Mehendale S, et al. Antioxidant effects of ginsenoside Re in cardiomyocytes. Eur J Pharmacol. 2006;532(3):201–7.
28. Ahn EH, Kang SS, Liu X, Chen G, Zhang Z, Chandrasekharan B, et al. Initiation of Parkinson's disease from gut to brain by delta-secretase. Cell Res. 2020;30(1):70–87.
29. Ahn EH, Liu X, Alam AM, Kang SS, Ye K. Helicobacter hepaticus augmentation triggers Dopaminergic degeneration and motor disorders in mice with Parkinson's disease. Mol Psychiatry. 2023;28(3):1337–50.
30. Ćulafić ĐM, Mirković DS, Vukčević MD, Rudić JS. Plasma and platelet serotonin levels in patients with liver cirrhosis. World J Gastroenterol: WJG. 2007;13(43):5750.
31. Miyata K, Shimokawa H, Higo T, Yamawaki T, Katsumata N, Kandabashi T, et al. Sarpogrelate, a selective 5-HT2A serotonergic receptor antagonist, inhibits serotonin-induced coronary artery spasm in a porcine model. J Cardiovasc Pharmacol. 2000;35(2):294–301.
32. Lu Q, Leong S, Lee KA, Patel A, Chua JME, Venkatanarasimha N, et al. Hepatic venous-portal gradient (HVPG) measurement: pearls and pitfalls. Br J Radiol. 2021;94(1124):20210061.
33. Li N, Tan S, Wang Y, Deng J, Wang N, Zhu S, et al. Akkermansia muciniphila supplementation prevents cognitive impairment in sleep-deprived mice by modulating microglial engulfment of synapses. Gut Microbes. 2023;15(2):2252764.
34. Ou Z, Deng L, Lu Z, Wu F, Liu W, Huang D, et al. Protective effects of Akkermansia muciniphila on cognitive deficits and amyloid pathology in a mouse model of Alzheimer's disease. Nutr Diabetes. 2020;10(1):12.
35. Saboo K, Petrakov NV, Shamsaddini A, Fagan A, Gavis EA, Sikaroodi M, et al. Stool microbiota are superior to saliva in distinguishing cirrhosis and hepatic encephalopathy using machine learning. J Hepatol. 2022;76(3):600–7.
36. Depommier C, Van Hul M, Everard A, Delzenne NM, De Vos WM, Cani PD. Pasteurized Akkermansia muciniphila increases whole-body energy expenditure and fecal energy excretion in diet-induced obese mice. Gut Microbes. 2020;11(5):1231–45.
37. Lawenius L, Scheffler JM, Gustafsson KL, Henning P, Nilsson KH, Collden H, et al. Pasteurized Akkermansia muciniphila protects from fat mass gain but not from bone loss. Am J Physiol Endocrinol Metab. 2020;318(4):E480–91.
38. Wen Y, Emontzpohl C, Xu L, Atkins CL, Jeong JM, Yang Y, et al. Interleukin-33 facilitates liver regeneration through serotonin-involved gut-liver axis. Hepatology. 2023;77(5):1580–92.
39. Choi W, Namkung J, Hwang I, Kim H, Lim A, Park HJ, et al. Serotonin signals through a gut-liver axis to regulate hepatic steatosis. Nat Commun. 2018;9(1):4824.
40. Ebrahimkhani MR, Oakley F, Murphy LB, Mann J, Moles A, Perugorria MJ, et al. Stimulating healthy tissue regeneration by targeting the 5-HT2B receptor in chronic liver disease. Nat Med. 2011;17(12):1668–73.
41. Kyritsi K, Chen L, O'Brien A, Francis H, Hein TW, Venter J, et al. Modulation of the Tryptophan Hydroxylase 1/Monoamine Oxidase-A/5-Hydroxytryptamine/5-Hydroxytryptamine Receptor 2A/2B/2C Axis Regulates Biliary Proliferation and Liver Fibrosis During Cholestasis. Hepatology. 2020;71(3):990–1008.
42. Vorobioff J, Garcia-Tsao G, Groszmann R, Aceves G, Picabea E, Villavicencio R, et al. Long-term hemodynamic effects of ketanserin, a 5-hydroxytryptamine blocker, in portal hypertensive patients. Hepatology. 1989;9(1):88–91.

43. Borcsiczky D, Szalay F, Tekes K, Tarcali J, Magyar K, de Châtel R. Platelet serotonin (5-HT) content is decreased in patients with alcoholic liver cirrhosis, but elevated in Gilbert's syndrome. J Hepatol. 1996;25(5):781–2.
44. Ponziani FR, De Luca A, Picca A, Marzetti E, Petito V, Del Chierico F, et al. Gut Dysbiosis and Fecal Calprotectin Predict Response to Immune Checkpoint Inhibitors in Patients With Hepatocellular Carcinoma. Hepatol Commun. 2022;6(6):1492–501.
45. Ponziani FR, Picca A, Marzetti E, Calvani R, Conta G, Del Chierico F, et al. Characterization of the gut-liver-muscle axis in cirrhotic patients with sarcopenia. Liver Int. 2021;41(6):1320–34.
46. Liu R, Kang JD, Sartor RB, Sikaroodi M, Fagan A, Gavis EA, et al. Neuroinflammation in Murine Cirrhosis Is Dependent on the Gut Microbiome and Is Attenuated by Fecal Transplant. Hepatology. 2020;71(2):611–26.
47. Bajaj JS, Salzman N, Acharya C, Takei H, Kakiyama G, Fagan A, et al. Microbial functional change is linked with clinical outcomes after capsular fecal transplant in cirrhosis. JCI Insight. 2019;4(24):e133410.
48. Han H, Yi B, Zhong R, Wang M, Zhang S, Ma J, et al. From gut microbiota to host appetite: gut microbiota-derived metabolites as key regulators. Microbiome. 2021;9(1):162.
49. Wu Z, Xu Q, Gu S, Chen Y, Lv L, Zheng B, et al. Akkermansia muciniphila Ameliorates Clostridioides difficile Infection in Mice by Modulating the Intestinal Microbiome and Metabolites. Front Microbiol. 2022;13: 841920.

Publisher's Note